

## Supplementary Materials for

### **Follicular CD8 T cells accumulate in HIV infection and can kill infected cells in vitro via bispecific antibodies**

Constantinos Petrovas,\* Sara Ferrando-Martinez, Michael Y. Gerner, Joseph P. Casazza, Amarendra Pegu, Claire Deleage, Arik Cooper, Jason Hataye, Sarah Andrews, David Ambrozak, Perla M. Del Río Estrada, Eli Boritz, Robert Paris, Eirini Moysi, Kristin L. Boswell, Ezequiel Ruiz-Mateos, Ilias Vagios, Manuel Leal, Yuria Ablanedo-Terrazas, Amaranta Rivero, Luz Alicia Gonzalez-Hernandez, Adrian B. McDermott, Susan Moir, Gustavo Reyes-Terán, Fernando Docobo, Giuseppe Pantaleo, Daniel C. Douek, Michael R. Betts, Jacob D. Estes, Ronald N. Germain, John R. Mascola, Richard A. Koup

\*Corresponding author. Email: petrovasc@mail.nih.gov

Published 18 January 2017, *Sci. Transl. Med.* **9**, eaag2285 (2017)  
DOI: 10.1126/scitranslmed.aag2285

#### **This PDF file includes:**

##### Materials and Methods

Fig. S1. T cell dynamics in HIV-infected LNs.

Fig. S2. Representative example of the histo-cytometry analysis.

Fig. S3. Dynamics of fCD8 with respect to HIV antigen distribution and collagen deposition in the LN areas.

Fig. S4. Gene signatures of sorted tissue CD8 T cell populations.

Fig. S5. Expression of exhaustion markers in fCD8 T cells.

Fig. S6. Expression of PD-1 in fCD8 T cells.

Fig. S7. Functionality of fCD8 T cells.

Fig. S8. Localization of GrzB<sup>+</sup> CD8 T cells in the GC.

Fig. S9. fCD8 T cells can mediate in vitro bispecific antibody killing.

Table S1. Demographic (age and gender) and clinical (CD4 counts, pVL, and treatment) data of the donors as well as the type of assay used for their tissue analysis are shown.

References (52–59)

## **Supplementary Materials**

### **Materials and Methods**

#### **Ethics statement**

The Institutional Review Boards at the relevant institutions approved lymph node extraction from HIV<sup>-</sup> and HIV<sup>+</sup> individuals. Signed informed consent was obtained before all procedures in accordance with the Declaration of Helsinki and approved by the appropriate Institutional Review Board. Tonsils were obtained from anonymized discarded pathologic specimens from Children's National Medical Center (CNMC) under the auspices of the Basic Science Core of the District of Columbia Developmental Center for AIDS Research. The CNMC Institutional Review Board determined that study of anonymized discarded tissues did not constitute 'human subjects research.' HIV<sup>+</sup> anonymized lymph node tissues were obtained from "Instituto Nacional de Enfermedades Respiratorias", Mexico City, Mexico and "Virgen del Rocio University hospital" (HUVR/IBiS/US), Sevilla, Spain. Cells and tissues from anonymized HIV<sup>-</sup> individuals were obtained from "Centre Hospitalier Universitaire Vaudois" (CHUV), Lausanne, Switzerland and the Pathology Department, General Hospital of Heraklion Crete, Greece. HIV-negative individuals were biopsied only for diagnostic purposes.

#### **Processing of tissues**

Upon receipt of tissue, lymph nodes and tonsils were washed with ice-cold medium R-10 (RPMI 1640 supplemented with 10% fetal bovine serum, 2 mM L-glutamine, 100 U/mL penicillin and 100 µg/mL streptomycin (Invitrogen). The surrounding fatty tissue was removed; tissues were cut into small pieces and then transferred to "C" tubes (Miltenyi) containing 5 ml of R-10 media. Cell suspensions were prepared with the aid of a GentleMACS cell dissociator (Miltenyi) and filtered through a 70 mm nylon

mesh (BD Biosciences). Cells were then counted and frozen at  $10 \times 10^6$  cells/ml of freezing media (10% DMSO in fetal bovine serum) (Lonza). Part of each lymph node biopsy was immediately placed in fixative (4% neutral buffered paraformaldehyde) and dedicated for paraffin embedded blocks followed by sectioning and analysis by multiplex confocal microscopy.

## **Antibodies**

**Flow cytometry:** directly conjugated antibodies were acquired from: (1) BD Biosciences: CD3-H7APC (clone SK7), CXCR5-Alexa488 (clone RF852), CCR7-Alexa700 (clone 150503), CD8-Pacific Blue (clone RPA-T8), CD4-APC (clone RPA-T4), IFN- $\gamma$ -PE (clone XMG1.2), CD160-PE (clone BY55), 2B4-BV421 (clone 2-69), CD4-BV605 (clone L200), IL-2 PerCP-Cy55 (clone MQ1-17H12) and MIP-1 $\beta$ -Cy7PE and -PE (clone D21-1351) (2) Beckman Coulter: CD45RO-ECD (clone UCHL1) and CD27-PC5 (clone 1A4CD27) (3) Biolegend: PD-1-BV711 (clone EH12.2H7), CCR7-BV605 (clone G043H7), TIM3-Cy7PE (clone F38-2E2), CD27-BV605 (clone O323), CD8-BV570 (clone RPA-T8) and perforin (Prf)-PE (clone B-D48) (4) Invitrogen: CD4-Cy5.5-PE (clone S3.5), CD4-QD605 (clone 53.5) and granzyme B (GrzB) -Cy5.5-PE (clone GB11) (5) eBiosciences: TIGIT-APC (clone MBSA43). TNF- $\alpha$ -Alexa594 or -PE (clone MAb11) was conjugated in-house. Quantum dots and Aqua amine viability dye were obtained from Invitrogen.

**Confocal microscopy:** Directly conjugated antibodies against CD20-eFluor615 (clone L26, eBiosciences), Ki67-Alexa700 or FITC (clone B56, BD Biosciences), CXCR5-APC (clone 51505, R&D), CD4-Alexa 488 (polyclonal goat IgG, R&D) and PD-1-Alexa 488 (polyclonal goat IgG, R&D) were used. Non-conjugated antibodies against p24 (clone Kal-1, DAKO), IgD (clone EPR6146, abcam), GrzB (clone GrB-7, Dako), CD8 (4B11, Thermo Scientific) CD4 (clone EPR6855, Abcam), were used in combination with appropriate secondary antibodies; anti-mouse IgG1-Alex546 (Life Technologies), anti-rabbit IgG-BV421 (Biolegend), anti-mouse IgG2a-Alex488 (Life Technologies) for the detection of

GrzB, anti-mouse IgG2b-Alexa546 (Life Technologies) for the detection of CD8 and anti-rabbit IgG-BV421 (Biolegend) for the detection of CD4. JoJo-1 (Invitrogen), a nucleic acid binding fluorescent dye (max ~545 nm) was used for nuclear staining.

### **Polychromatic flow cytometry**

**Phenotypic analysis:**  $1-2 \times 10^6$  cells were thawed out and rested for 2h in a cell culture incubator before further use. Fresh tonsil-derived cells were also used for some experiments. Cells were incubated with a viability dye (Aqua-dye, Invitrogen) and surface stained with titrated amounts of antibodies against CD3, CD4, CD8, CD27, CD45RO, CCR7, CXCR5 and PD-1. Titrated amounts of antibodies against TIM3, CD160, TIGIT, and 2B4 were used in combination with the previous monoclonal antibodies to analyze the frequency of co-stimulatory and co-inhibitory receptors. Following a washing step, cells were fixed with 1% paraformaldehyde.

**Functional analysis:**  $1-2 \times 10^6$  cells were used for the *ex vivo* detection of Grzb and Prf. Cells were surfaced stained with Aqua and titrated amounts of antibodies against CD4, CD8, CCR7 and CXCR5. After a washing step, cells were fixed and permeabilized (Cytotfix/Cytoperm kit; BD Biosciences) and stained with anti-CD3, anti-GrzB and anti-Prf antibodies. Use of the B-D48 anti-human Prf clone allows for the measurement of the newly, de novo produced cytolytic molecule (44, 45). For the *de novo* production of cytokines, cells were stimulated with anti-CD3/CD2/CD28 beads (Myltenyi) or HIV-1 Gag-peptide pools (15mers overlapping by 11 residues; National Institutes of Health AIDS Research and Reference Reagent Program). Cell were stimulated for 6h in the presence of brefeldin A in R-10 (10  $\mu$ g/ml; Sigma-Aldrich), washed and permeabilized (Cytotfix/Cytoperm kit; BD Biosciences).

Intracellular staining was also carried out using titrated antibodies against CD3, IFN- $\gamma$ , TNF- $\alpha$  and MIP-1 $\beta$ . Between 500,000 and  $1 \times 10^6$  events were collected in each case on a modified LSRII flow cytometer (BD Immunocytometry Systems). Electronic compensation was performed with antibody capture beads

(BD Biosciences). Data were analyzed using FlowJo Version 9.7 (TreeStar). Forward scatter area vs. forward scatter height was used to gate out cell aggregates.

### ***In vitro* PD-1/PDL-1 blocking assay**

Tonsil-derived cells were stimulated by plate-bound anti-CD3 (clone UCHT1, functional grade, BD, Cat. No 16-0038, at 0.1 and 0.5 µg/ml) in the presence of isotype (IgG1, ebioscience) or anti-PD-L1 (clone MIH1, functional grade, ebioscience, Cat. No 16-5982-82, at 15ug/ml) or anti-PD-1 (clone J116, functional grade, ebioscience, Cat. No. 14-9989-82, at 15 ug/ml) for 5 days. On the harvesting day, cells were incubated with brefeldin A for 6h and the cytokine production was measured by intracellular staining. Briefly, cells were washed and stained with aqua and antibodies against surface markers (CD4, CD8, CD27, CD45RO). Following a fixation/permeabilization step (Cytotfix/Cytoperm kit; BD Biosciences), cells were stained with CD3, IFN- $\gamma$ , TNF- $\alpha$  and IL-2 antibodies, fixed and events were collected on a modified LSRII flow cytometer.

### **Imaging studies**

6-10 µm formalin fixed, paraffin embedded sections were deparaffinized and rehydrated in deionized water. Epitope retrieval was performed using a decloaking chamber (Biocare Medical) (125°C, 30 sec) with Borg (for paraffin slides) Decloaker buffer (Biocare Medical) followed by a cooling step to room temperature. Following blocking for 1 hour (0.1M Tris, 0.3% Triton X-100, 1% Bovine Serum Albumin) sections were stained with titrated amounts of non-conjugated antibodies (GrzB, CD4, CD8, IgD, p24). Following an overnight incubation at 4<sup>0</sup>C, slides were washed with PBS (3 x 20 min) and stained with the appropriate secondary antibodies for 2 hours at room temperature (RT). Slides were washed and, after another blocking step for 1 hour (RT) with a 1:1 mixture of normal mouse serum and purified IgG2b (clone eBMG2b, eBioscience) antibody (for panels including both CD8 and CXCR5) or with a 1:10 dilution of normal mouse serum, were stained for 2 hours (RT) with titrated amounts of

conjugated antibodies (PD-1, CD20, Ki67, CXCR5). A final washing step and Jojo staining were performed before mounting the slides with Fluoromount G (SouthernBiotech). Slides were imaged with a Leica SP8 or Nikon C2si confocal microscope using a 20x 0.75 NA or 40x 1.30 NA objective with a 1.5x optical zoom at a 1024x1024 pixel density. For some images a 63x 1.40 NA objective was used. Multi-parameter confocal microscopy images were then analytically processed via the Histo-cytometry pipeline (32) with minor modifications. In brief, fluorophore spillover was first corrected by imaging single-stained tissues and creating a compensation matrix via the Leica LAS-AF Channel Dye Separation module (Leica Microsystems). Spillover corrected images were then analyzed with Imaris software (Bitplane Scientific). 3-dimensional segmented surfaces representing either the CD8<sup>+</sup> T cell membranes (using the CD8 signal) or all imaged cells (using the nuclear signal) were generated via the Surface Creation module. Average voxel intensities for all channels of interest, such as PD-1 or CXCR5, within these surfaces, along with the X, Y positioning of the cell centroids, were then exported to Excel and combined into a unified spreadsheet file (comma separated values format). This spreadsheet was then imported into Flowjo vX0.7 program for further analysis. In some experiments, cellular distances to B cell follicles or germinal centers (GC) were determined. For this, the follicles or GC were marked within the images via the Spot Creation module (Imaris) and the X, Y coordinates for these spots were exported into the unified spreadsheet file. Cellular distances to follicles or GC were then calculated by determining the minimal distances between each cell (nuclear segmentation) or CD8 T cells (CD8 membrane segmentation) and the follicle/GC representative spots. In some analyses, the ratio of CD4<sup>+</sup> or CD8<sup>+</sup> T cells to GC area was quantified. For this, manual analysis of the GC area and CD4<sup>+</sup> vs. CD8<sup>+</sup> infiltration was conducted in Imaris, with the ratios quantified in Excel. All additional statistical analysis and graphing were performed using Prism (GraphPad). Presented confocal images are maximum projections of 3-5 separate confocal Z slices.

## **Quantification of Collagen-1, CD8 and CD20 in LN sections**

Multiplexed fluorescence was performed using the Opal TSA system (Perkin Elmer) with minor modifications from what was previously described (52). Briefly, 5µm LN section slides were baked at 60°C for 1 hour, put in xylene for 10 min then rehydrated in graded ethanols (100%-70%) then placed in double-distilled water. Antigen retrieval was performed in 0.01% citraconic anhydride (CA) with 0.05% Tween-20 (pH 7.4; Sigma) using pressure cooker at 122°C for 30 seconds. Tissues were incubated with rabbit monoclonal anti-CD8 (1:1,000; clone SP16; ThermoFisher) overnight at room temperature, washed in 1x Tris-buffered saline (TBS; Boston BioProducts) containing 0.05% Tween-20 (TBS-Tw), followed incubation with a biotin-free polymer anti-rabbit HRP system (Rabbit Polink-1, Golden Bridge International, Inc.) for 15 min at room temperature. Visualization of CD8+ cells was performed using the OPAL 520 substrate. Following CD8 detection, slides were placed in a pressure cooker in CA retrieval buffer at 122°C for 30 seconds followed by incubation with mouse monoclonal anti-CD20 (1:2,000; clone L26; Dako) for 1 hour at room temperature and detected using the biotin-free polymer anti-mouse HRP system (Mouse Polink-1, Golden Bridge International, Inc.) and visualized by using OPAL 690. Following CD20 detection, slides were placed in a pressure cooker in CA retrieval buffer at 122°C for 30 seconds then treated with proteinase K (4ug/ml) for 20 min at room temperature followed by incubation with mouse monoclonal anti-Collagen-1 (1:2000; clone COL-1; Sigma) for 1 hour at room temperature and visualized using the biotin-free polymer anti-mouse HRP system (Mouse Polink-1, Golden Bridge International, Inc.) and OPAL 590. Slides were counterstained with DAPI (Perkin Elmer) for 10min, washed in TBS-Tw and cover slipped with #1.5 GOLD SEAL® cover glass (EMS) using Prolong® Gold reagent (Invitrogen). To quantify each marker, whole slides were scanned at 20× magnification with an Aperio FL Immunofluorescence Slide Scanner (Aperio Technologies), defined regions of interest (ROI) images extracted and analyzed using either Image J software or Photoshop CS5 with Fovea tools by measuring percent positive area within the defined ROIs.

## ***Ex vivo* sorting LN T<sub>FH</sub> cells and HIV DNA and RNA PCR assays**

PD-1<sup>dim</sup> and PD-1<sup>high</sup> T<sub>FH</sub> cells were sorted from viremic (n=4) and long-term cART (n=4) LNs and HIV RNA species and Gag DNA was measured by RT-PCR. Spliced and unspliced HIV RNAs were

measured using quantitative RT-PCR as described (56). Average gag DNA/cell was determined as described (54).

### **Whole Transcriptome Sequencing (mRNA-Seq)**

Memory non-fCD8 and fCD8 were sorted from viremic HIV+LNs (n=3) and tonsils (n=2) for whole transcriptome analysis. Non-strand-specific RNA-Seq libraries were prepared as described previously (57). Briefly, Polyadenylated transcripts were purified on oligo-dT magnetic beads, fragmented, reverse transcribed using random hexamers and incorporated into barcoded cDNA libraries based on the Illumina TruSeq platform. Libraries were validated by microelectrophoresis, quantified, pooled and clustered on Illumina TruSeq v2 flowcells. Clustered flowcells were sequenced on an Illumina HiSeq 2000 in 75bp paired-end reactions. The final dataset comprised  $3.54 \times 10^8$  75-bp read pairs in total, with each sample corresponding to about  $1 \times 10^7$  read pairs on average. RNA-seq data were submitted to The Gene Expression Omnibus (GEO) repository at the National Center for Biotechnology Information (NCBI). Trimmomatic (version 0.22) was used to remove adapters and low quality bases. The trimmed paired-end reads were aligned to hg19 reference genome by TopHat package (58), followed by Cufflinks for RNA expression analysis, and by Cuffdiff for differential gene expression analysis (59). In the process, five samples with concordant pair alignment rate less than 75% were excluded from further analysis. Differentially expressed genes were defined as those with false discovery rate  $< 0.05$ . GSEA (<http://www.broadinstitute.org/gsea/>, “c2.cp.v4.0.symbols.gmt.txt”) was used to identify the pathways enriched in differentially expressed genes (false discovery rate  $< 0.15$ ). The heatmap figures were generated by R package (“gplots”). The network figure of pathways and related genes was generated by cytoscape software (version 2.8.3).



## **Luminex assay**

Fresh tonsil CD8 T cells were sorted based on their expression of CD27, CD45RO, CCR7 and CXCR5. Following stimulation with anti-CD3/CD2/CD28 for 24h, supernatants were collected and the secreted amounts of sFasL, Prf and GrzB were measured by a commercially available multiplexed assay (Luminex, EMDmillipore).

## **Construction and purification of bispecific antibodies and controls**

The cDNAs for human VRC07-523 (Fab) were PCR amplified from the IgG vector and assembled to anti-human CD3 using overlapping PCR. The scFv fragment of an anti-human CD3 monoclonal antibody was linked by a 16 aa GS linker to the light chain of VRC07-523 and the VH/CH1 domains of VRC07-523 were kept intact to form the bispecific antibody. Anti-human CD3 scFv sequences were synthesized using human preferred codons (GenScript). Overlapping PCR was also employed to assemble the control bispecific antibody based on an anti-influenza antibody 9114. All bispecific antibodies were configured as Fab-scFv. Assembled cDNAs were cloned into mammalian expression vector for protein production using 293F cells. To produce large quantities of the bispecific antibodies, 293F cells were transfected with different bispecific expression vectors using 293Fectin according to the manufacturer's protocol (Life Technologies). Five days post-transfection, cell culture supernatant was harvested and filtered. The proteins were initially purified using Kappaselect beads (GE Healthcare Biosciences), followed by gel-filtration using a HiLoad 16/600 Superdex 200 pg column (GE Healthcare Biosciences). Only the monomer fractions were collected for further characterization. The endotoxin level of all purified antibodies was measured and samples with high levels of endotoxin were passed through an endotoxin-removal column (Hyglos). The endotoxin level in all samples used in the *in vitro* and *in vivo* studies was <1 EU/mg.

### ***In vitro* killing assays**

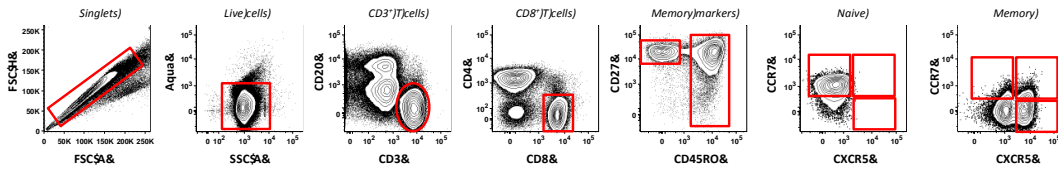
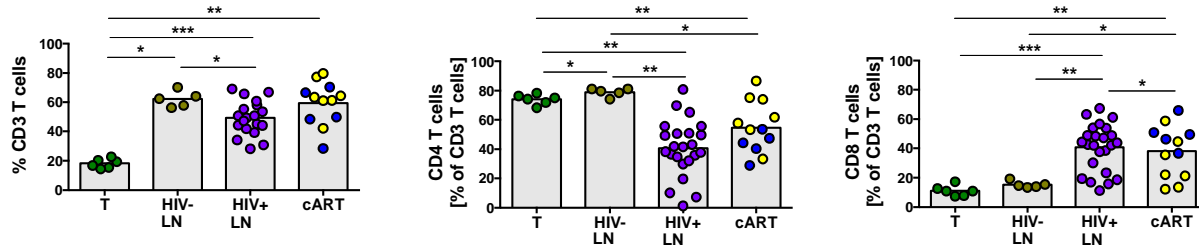
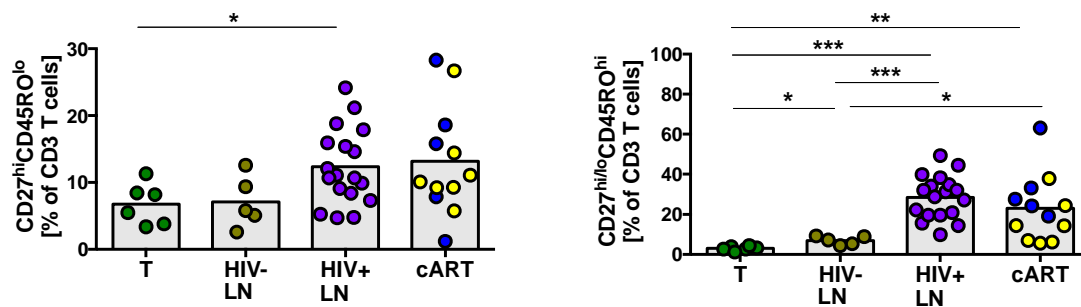
***Cell line (CEM-NKR-CCR5) targets:*** CD8 T cells from tonsils or HIV<sup>+</sup> viremic lymph nodes were sorted based on their expression of CD27, CD45RO, CCR7 and CXCR5 and co-cultured with labeled (PKH, Sigma-Aldrich) CEM ([https://www.aidsreagent.org/reagentdetail.cfm?t=cell\\_lines&id=29](https://www.aidsreagent.org/reagentdetail.cfm?t=cell_lines&id=29)) infected with HIV-IIIIB virus, (infectivity was routinely >90%) in the presence of a control (anti-CD3/isotype) or specific (anti-CD3/VRC07) bispecific antibody (500 ng/mL). Cells were harvested, washed and stained with Aqua and annexin V. The % of Lysis was calculated based on the Aqua<sup>-</sup>annexin V<sup>-</sup> and Aqua<sup>+</sup>annexin V<sup>+</sup> (necrotic and/or late apoptotic) and Aqua<sup>-</sup>annexin V<sup>+</sup> (early apoptotic) cell ratios. For some experiments, CEM cells were pre-incubated with 50uM z-VAD (Tocris Bioscience), a pan-caspase inhibitor, for 2h prior the co-culture with CD8 T cells. The supernatants of some co-cultures were analyzed for secreted sFasL, GzB and Prf using a multiplexed assay (Luminex, EMD millipore).

***Primary CD4 T cell targets:*** total memory CD4 and CD8 T cells were sorted from HIV<sup>-</sup> PBMCs (n=2). CD4 T cells were infected with a replication-competent, CXCR4-tropic, GFP-encoding virus (NL4-3) by mixing with the viral stock at an m.o.i. of 0.1 as previously described (53). Briefly, cells were stimulated (PHA), rested and infected for 2h at 37C, washed twice with media and cultured for 4d in the presence of IL-2 (40U/ml, Peprotech). Autologous CD8 T cells were cultured in the presence of IL-2 (5U/ml). Infected CD4 and CD8 T cells were co-cultured (at a ratio of 1:2) for 8h in the presence of anti-CD3/isotype or anti-CD3/VRC07 (300 ng/ml), washed and stained for aqua, annexin V and CD4. After fixation, events were collected on LSRII. Alternatively, sorted PD-1<sup>high</sup> T<sub>FH</sub> cells and memory CD8 T cells from HIV<sup>-</sup> tonsils (n=3) were used. CD4 T cells were infected without stimulation as described above. Infected CD4 and autologous CD8 T cells were co-cultured for 8h in the presence of anti-CD3/isotype or anti-CD3/VRC07 (300 ng/ml) and *in vitro* killing activity was measured.

## **Virus production assay**

T<sub>FH</sub> and fCD8 T cells were sorted from viremic HIV<sup>+</sup> LNs (n=2); CD4 T cells were stimulated with anti-CD3 (5ul/ml, HIT3a, functional grade, BD, Cat. No 16-0039) and IL-2 (40U/ml) while fCD8 T cells were treated only with IL-2 for 48h (see Extended Data Figure 9E for experimental scheme). Stimulated CD4 T cells were washed (x3) to remove free virus and co-cultured with fCD8 at a 1:2 ratio in the presence of anti-CD3/isotype or anti-CD3/VRC07 antibodies (300 ng/ml). Supernatants were collected at 24 and 48h and HIV gag RNA was measured.

***Quantification of HIV gag RNA from culture supernatants:*** Culture supernatants were collected, distributed and stored frozen in 96-well plates. RNA was isolated from the thawed culture supernatant using the Beckman-Coulter RNAdvance Tissue Kit (A32646) followed by treatment with DNase I and heat DNase inactivation. HIV gag DNA PCR was performed to confirm elimination of HIV gag DNA for each individual isolation. Quantitative HIV gag RNA real-time RT-PCR was performed twice per RNA isolation using the Life Technologies Ultrasense One-Step RT-PCR Kit (11732-927) with HIV gag RNA standards and previously described primers and probe(54) at 0.625 μM and 0.2 μM, respectively. An internal RNA standard from the avian derived retrovirus RCAS was used to quantify RNA recovery for each isolation as previously described (55) and was on average 76% (range 60-91%). RNA recovery, the fraction of supernatant sampled for RNA isolation, the fraction of isolated RNA sampled for RT-PCR, and the number of copies of HIV gag RNA detected in the RT-PCR well was used to determine the HIV gag RNA copy number in each original culture well.

**A****B****C**

**Fig. S1. T cell dynamics in HIV-infected LNs.** (A) Gating strategy used to define non-follicular ( $CCR7^{hi}CXCR5^{lo}$ ) and follicular ( $CCR7^{lo}CXCR5^{hi}$ ) CD8 T cells in flow cytometry data sets. (B) Pooled data showing the relative frequency of CD3, CD4 and CD8 T cells in tonsils, HIV<sup>-</sup>, viremic HIV<sup>+</sup> lymph nodes and short-term (blue dots) and long-term (yellow dots) cART-treated HIV-infected lymph nodes. Results are showed as frequency of total CD3 T cells. Mann-Whitney U test; \* $p < 0.05$ , \*\* $p < 0.001$ , \*\*\* $p < 0.0001$ . (C) Frequency of naive ( $CD27^{hi}CD45RO^{lo}$ ) and memory ( $CD27^{hi/lo}CD45RO^{hi}$ ) CD8 T cells in tonsils, HIV<sup>-</sup> and HIV<sup>+</sup> lymph nodes (viremic and cART-treated). Results are showed as frequency of total CD3 T cells. Mann-Whitney U test; \* $p < 0.05$ , \*\* $p < 0.001$ , \*\*\* $p < 0.0001$ .

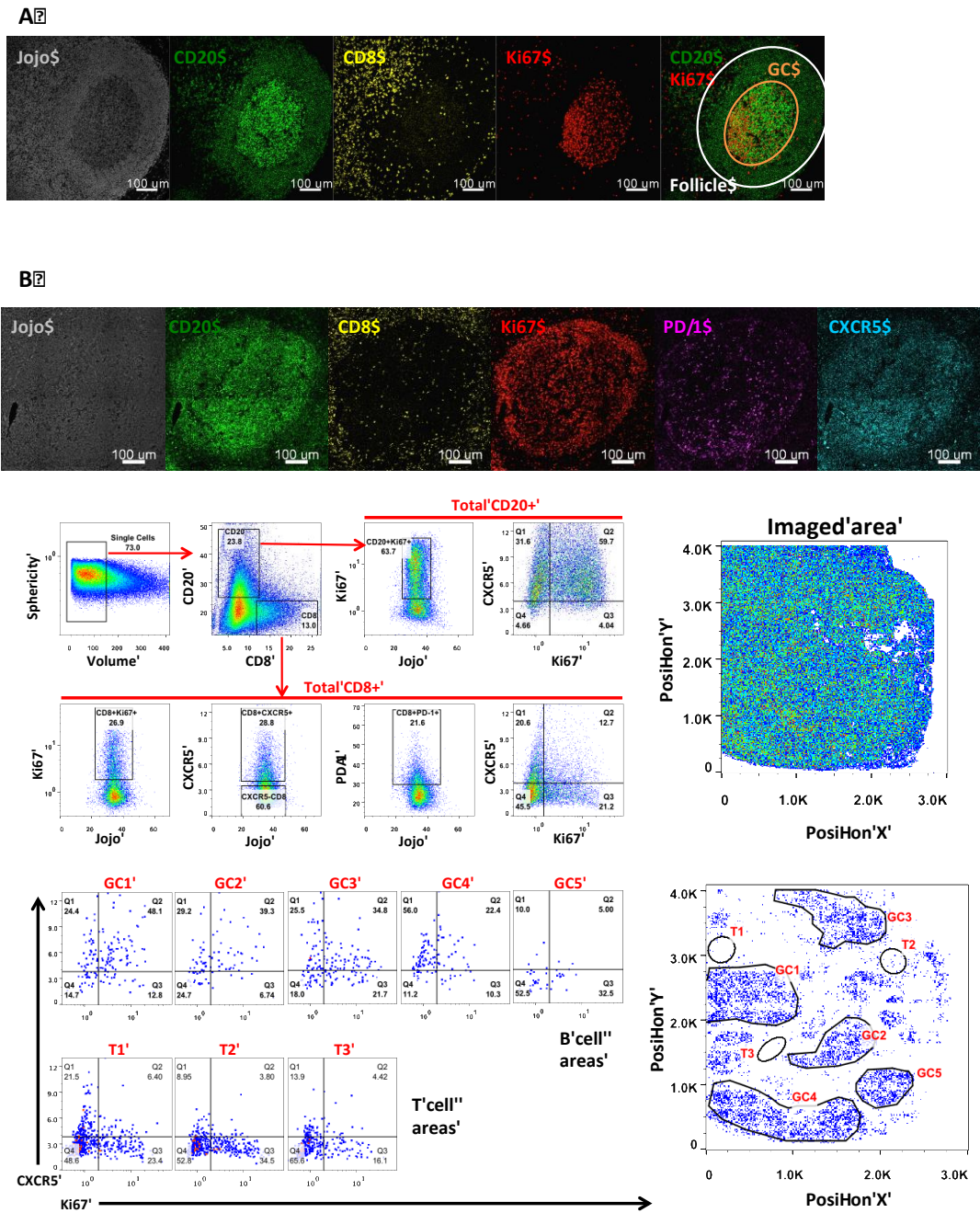


**Fig. S2. Representative example of the histo-cytometry analysis.** (A) Representative example of a 4-color staining panel used for confocal imaging. The B cell follicle with surrounding area from an HIV<sup>-</sup> LN is shown. The follicular (white circle) and GC area (CD20<sup>hi</sup>Ki67<sup>hi</sup>, orange circle) are also marked. (B) Representative example of a 6-color staining panel used for Histo-cytometry analysis is shown. Representative Histo-cytometry analysis of a viremic HIV<sup>+</sup> lymph node with the gating scheme for the detection of the indicated populations. The whole imaged area (position X, Y plot) (HIV<sup>+</sup> #22), the

expression of Ki67 and CXCR5 in total CD20 and the expression of Ki67, CXCR5 and PD-1 in total CD8 T cells are shown (*upper panel*). The frequency of CD8 T cells with respect to CXCR5 and Ki67 expression within the GCs and T cell areas (defined by high intensity of CD8 staining and rare CD20 signal) as well as the position of particular GCs (defined as CD20<sup>+</sup>Ki67<sup>+</sup>) are shown (*lower panel*).

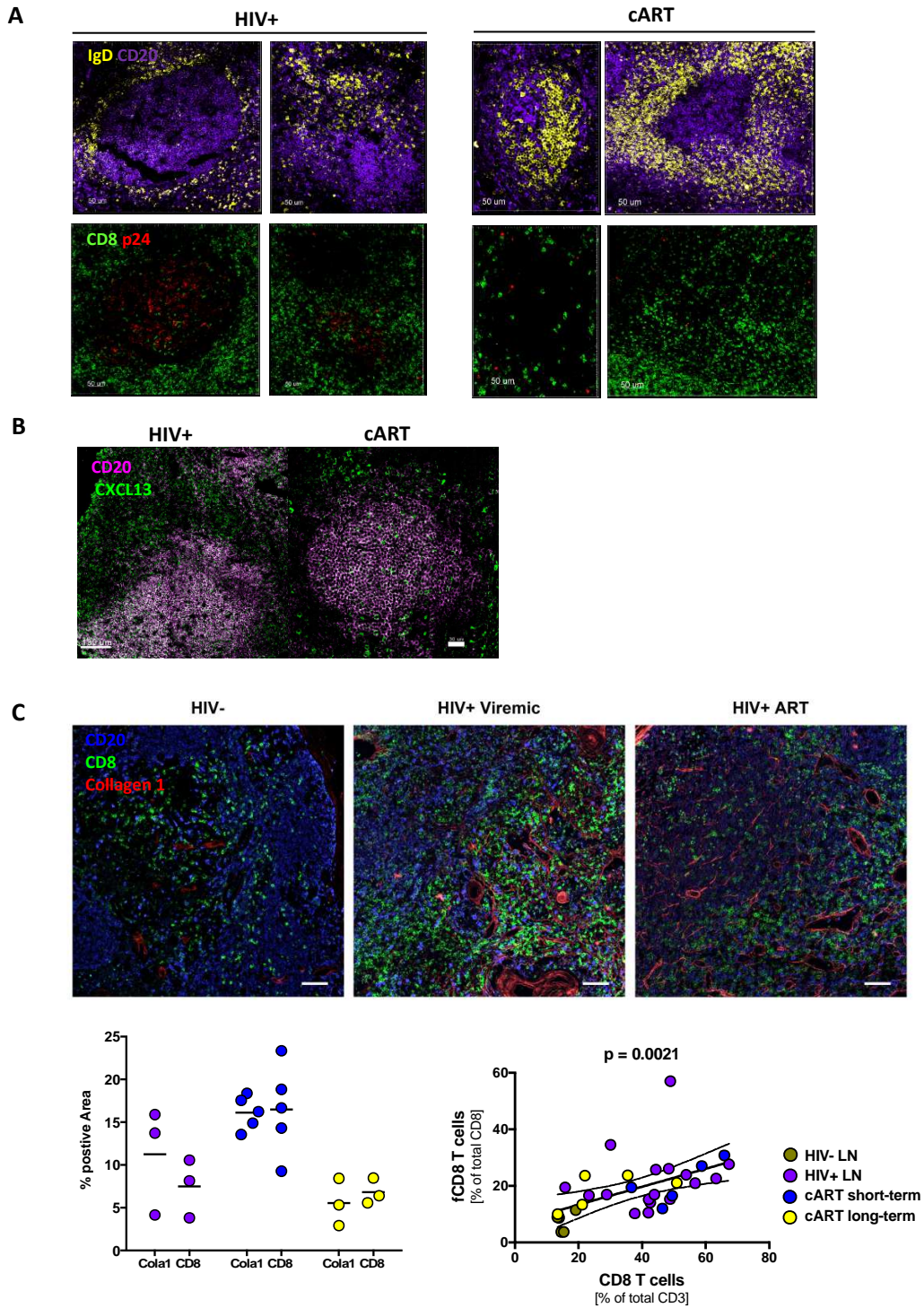


**Fig. S3. Dynamics of fCD8 with respect to HIV antigen distribution and collagen deposition in the LN areas.** (A) Representative confocal images (20X) from HIV<sup>+</sup> (n=2) and long-term cART (n=2) LNs showing the follicles (defined by IgD and CD20) and the distribution of CD8 and p24<sup>+</sup> cells in the follicular areas (lower panel). (B) representative images showing the expression of CXCL13 in follicular

(CD20<sup>hi</sup>) and non-follicular areas in HIV+ and cART LNs. and (C) Images showing the distribution of CD8 and collagen 1 in follicular and non-follicular areas from HIV-, HIV viremic and cART LNs (*upper panel*). Pooled data showing the frequency of CD8 T cells (expressed as frequency of the positive area for CD8) and fibrosis (expressed as frequency of the positive area for collagen 1) in chronic HIV viremic, short-term and long-term cART LNs (*lower left panel*). The correlation between total and fCD8 T cell frequencies is shown in the *lower right panel*. Linear regression,  $p = 0.0021$ .



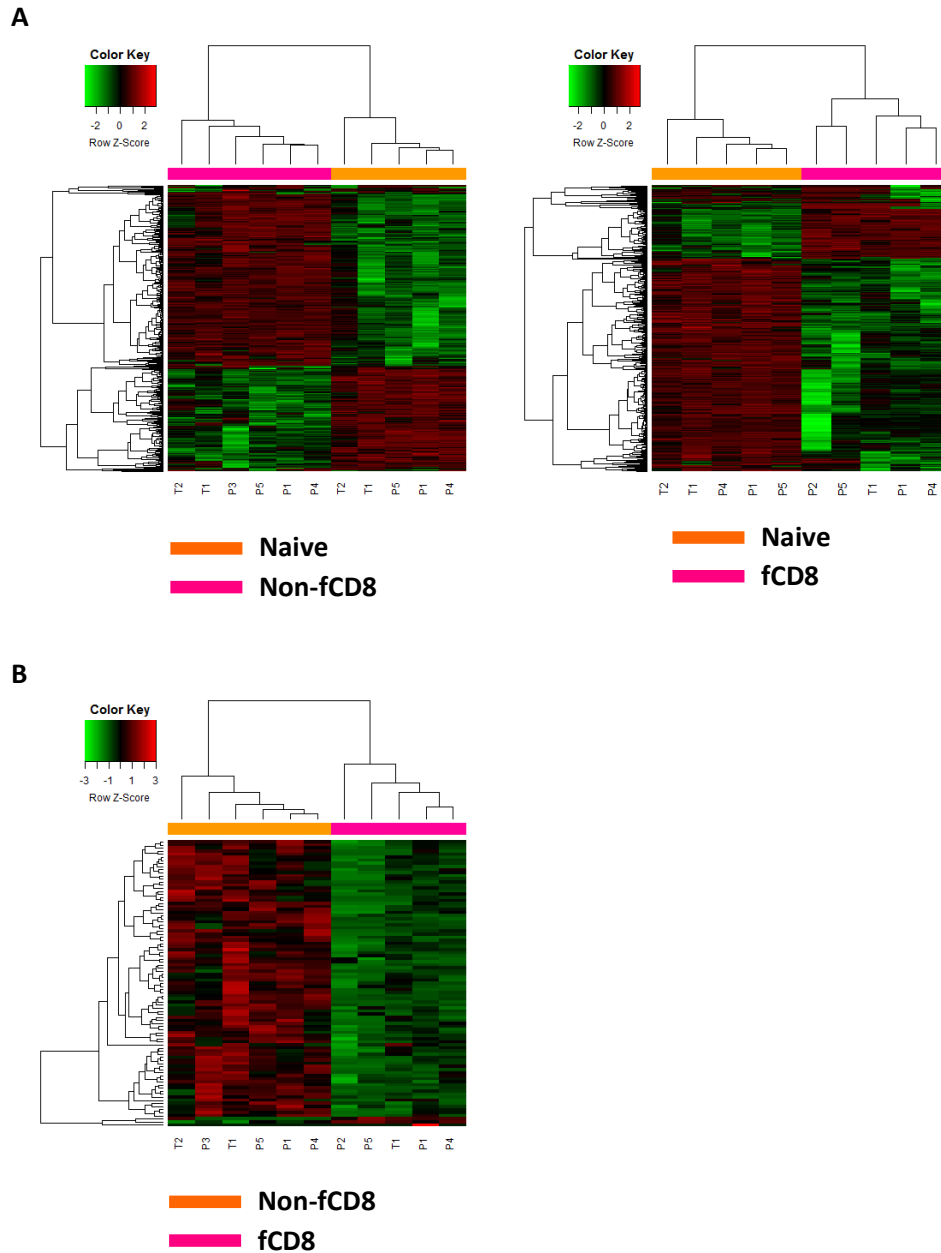


**Fig. S4. Gene signatures of sorted tissue CD8 T cell populations.** Heat map clustering analysis of gene expression for (A) naive vs non-fCD8 (*left panel*), naive vs fCD8 T cells (*right panel*) and (B) non-fCD8 vs fCD8 T cells. Only genes differently expressed between the cellular populations tested with false discovery rate  $<0.05$  were used to produce the Heatmap. Sorted cells from HIV<sup>+</sup> LNs (n=3) and tonsils (n=2) were used for the analysis.

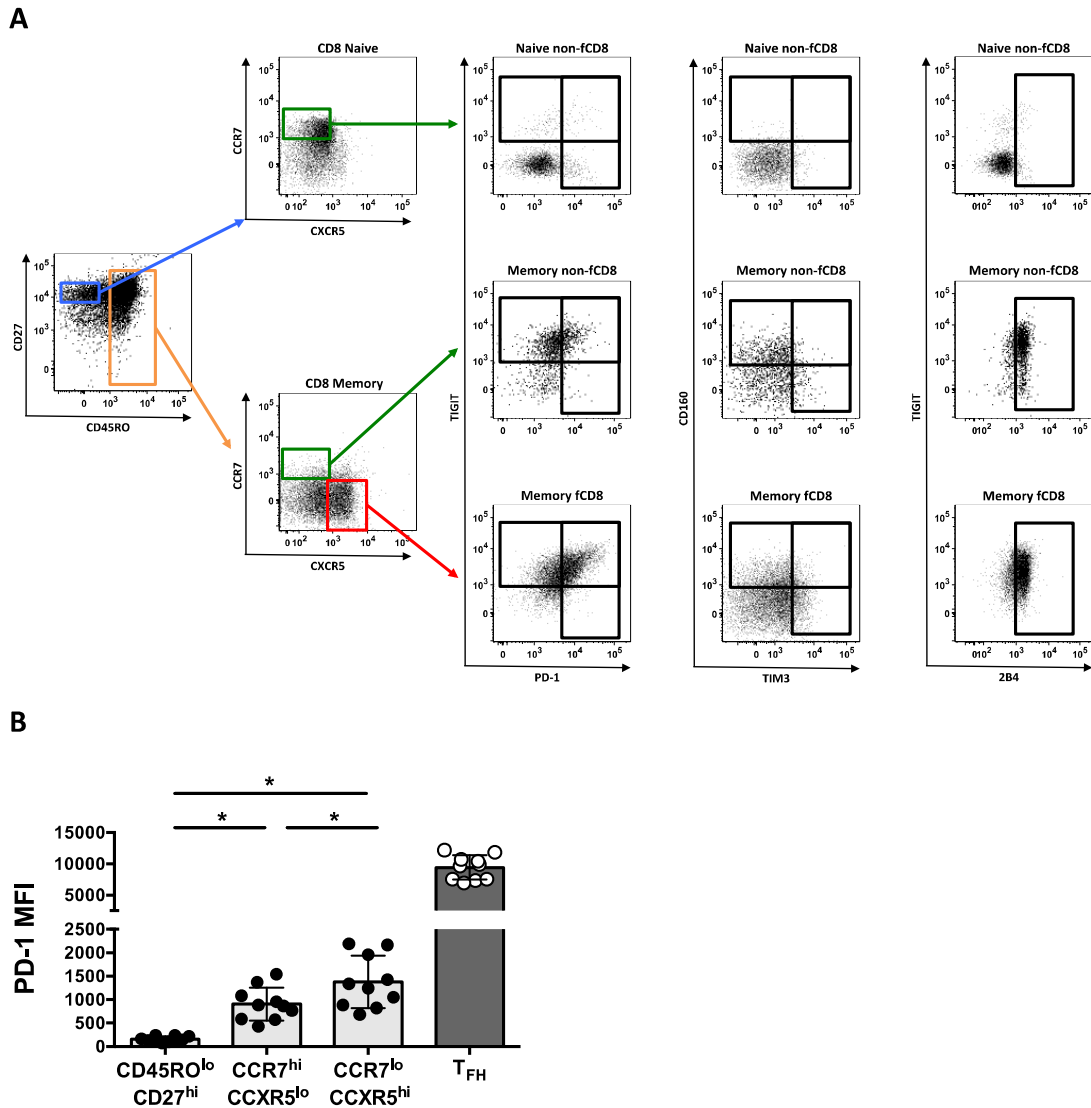


**Fig. S5. Expression of exhaustion markers in fCD8 T cells.** (A) Gating strategy used to analyze the expression of co-inhibitory receptors in naïve, non-fCD8 and fCD8. A representative viremic donor is shown. (B) MFI of the PD-1 expression among naïve CD8 (CD27<sup>hi</sup>CD45RO<sup>lo</sup>), non-fCD8 (CCR7<sup>hi</sup>CXCR5<sup>lo</sup>), fCD8 (CCR7<sup>lo</sup>CXCR5<sup>hi</sup>) and CD4 T<sub>FH</sub> (PD-1<sup>hi</sup>CXCR5<sup>hi</sup>) T cells, Wilcoxon signed-rank test; \*p < 0.05. ANOVA non-parametric test between CD8 Naive, non-fCD8 and fCD8 p < 0.0001.

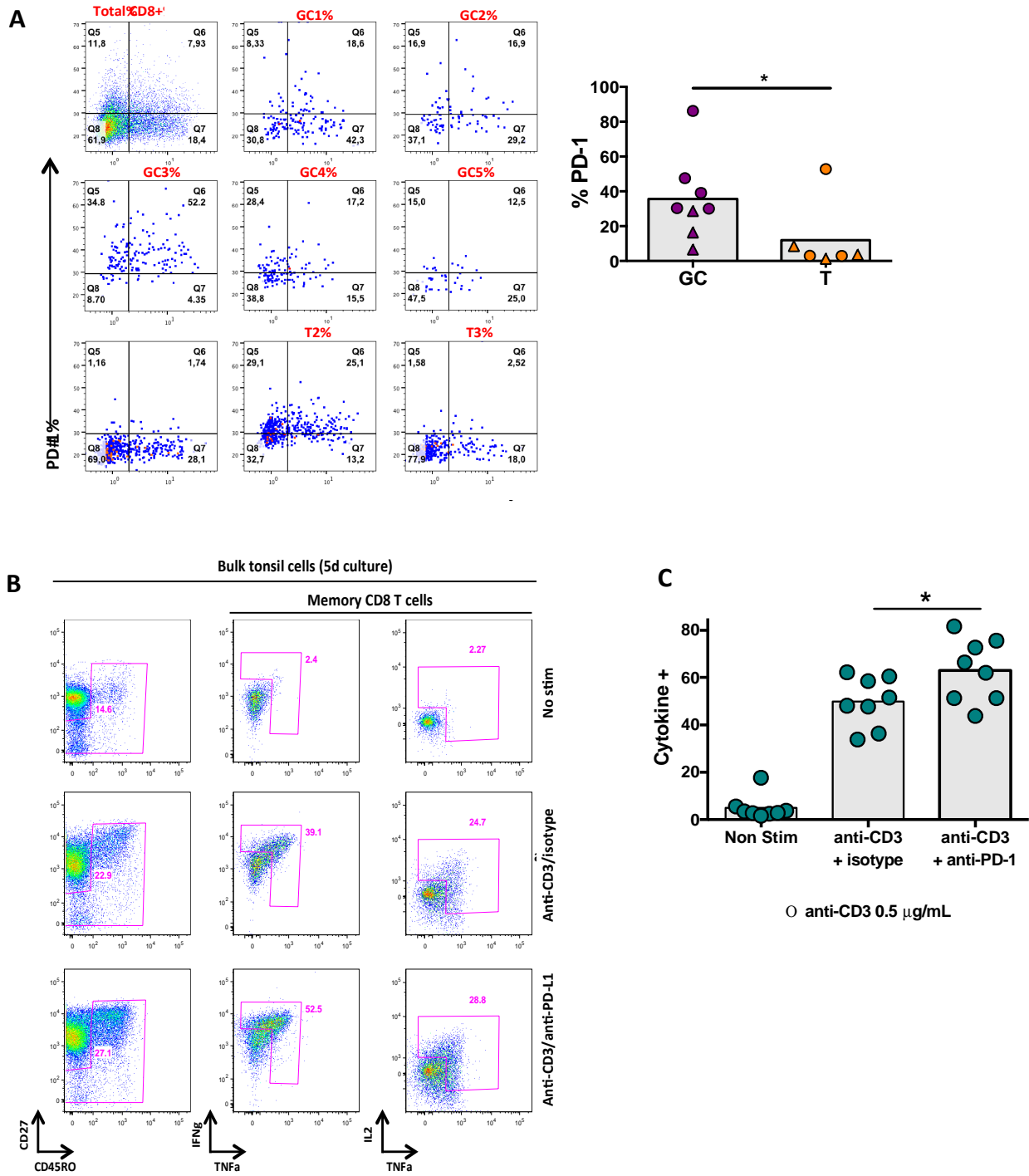
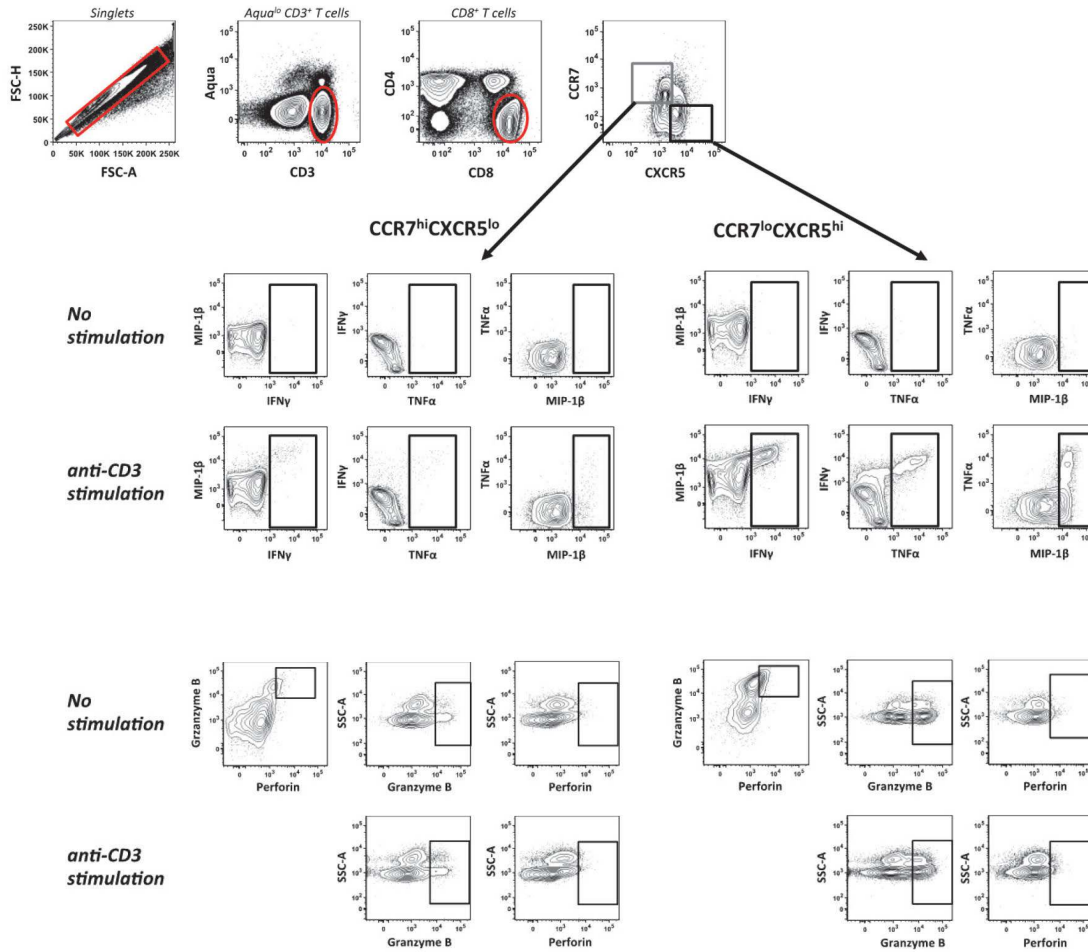


**Fig. S6. Expression of PD-1 in fCD8 T cells.** (A) Histo-cytometry plots showing the expression of PD-1 and Ki67 in total and CD8 T cells from individual GCs and T cell areas for a viremic HIV<sup>+</sup> lymph node (HIV+ #22) (*left panel*). Pooled data showing the frequency of PD-1<sup>hi</sup> CD8 T cells in GC and T cell areas from two viremic HIV<sup>+</sup> lymph nodes (right panel). Different symbols (circle, triangle) represent different patients while each dot represents a different B or T cell area. Mann-Whitney U test;

\* $p < 0.05$ . **(B)** Flow cytometry plots showing the naïve and memory compartments (based on the CD27 and CD45RO expression) and the cytokine production (IFN- $\gamma$  vs TNF- $\alpha$  and TNF $\alpha$  vs IL-2) by total memory CD8 T cells after 5 days stimulation in the absence or presence of anti-PD-L1. **(C)** Pooled data showing the cytokine production (IFN- $\gamma$  and/or TNF- $\alpha$  and/or IL-2) by memory CD4 T cells after 5 days incubation in the presence of absence of a blocking PD-1 antibody.

**A**



**B**

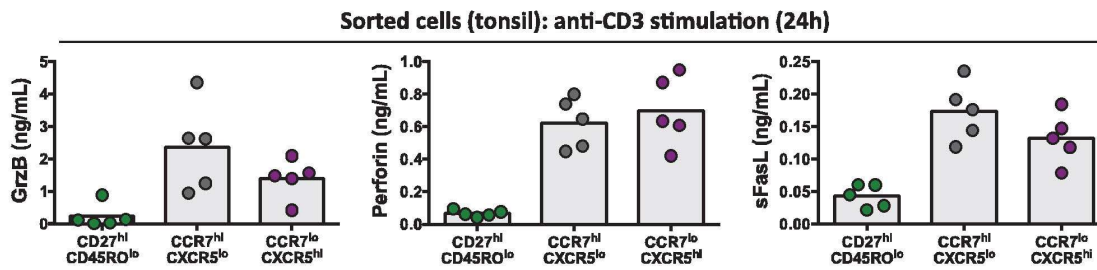


**Fig. S7. Functionality of fCD8 T cells.** (A) Gating strategy used to analyze cytokine (IFN- $\gamma$ , TNF- $\alpha$ ) and chemokine (MIP-1 $\beta$ ) production, and cytolytic activity (GrzB, Prf) of CD8 after 6h stimulation with anti-CD3/CD28 beads. (B) The concentration (measured by Luminex) of secreted GrzB, Prf and sFasL molecules by naive CD8 (CD27<sup>hi</sup>CD45RO<sup>lo</sup>), non-fCD8 (CCR7<sup>hi</sup>CXCR5<sup>lo</sup>) and fCD8

(CCR7<sup>lo</sup>CXCR5<sup>hi</sup>) sorted T cells from tonsils (n = 5) after 24h stimulation with anti-CD3/CD28 beads is shown.

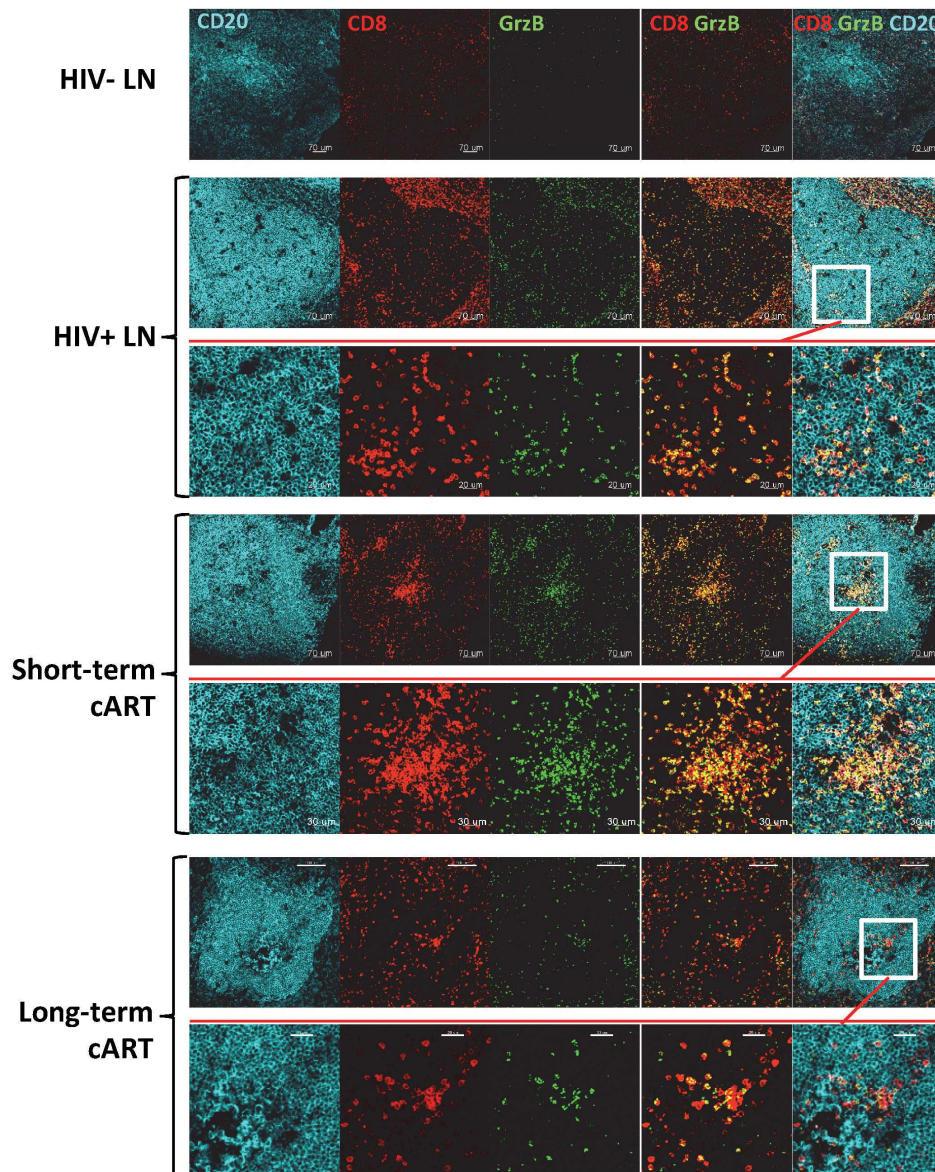
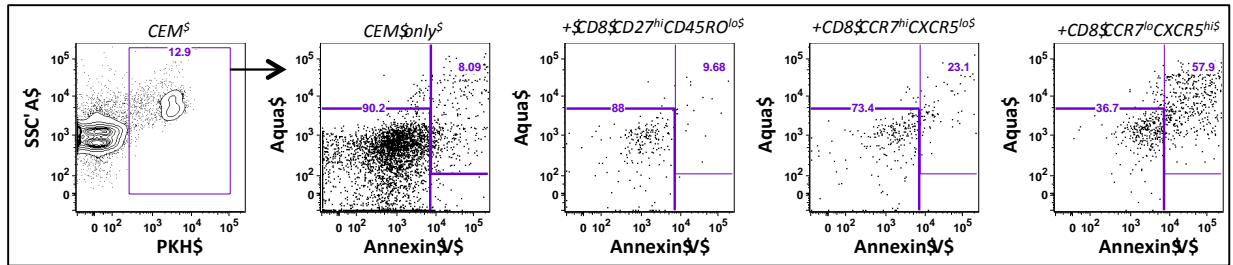


**Fig. S8. Localization of GrzB<sup>+</sup> CD8 T cells in the GC.** Representative confocal images of LNs from HIV<sup>-</sup>, viremic HIV<sup>+</sup> and cART-treated (short- and long-term treatment) HIV<sup>+</sup> individuals, stained for CD20, CD8 and GrzB. Individual staining as well as merged images (CD8/GrzB and CD20/CD8/GrzB) are shown. Zoomed images of the highlighted areas (white squares) show the presence of GrzB<sup>+</sup>CD8 T cells within the germinal center.

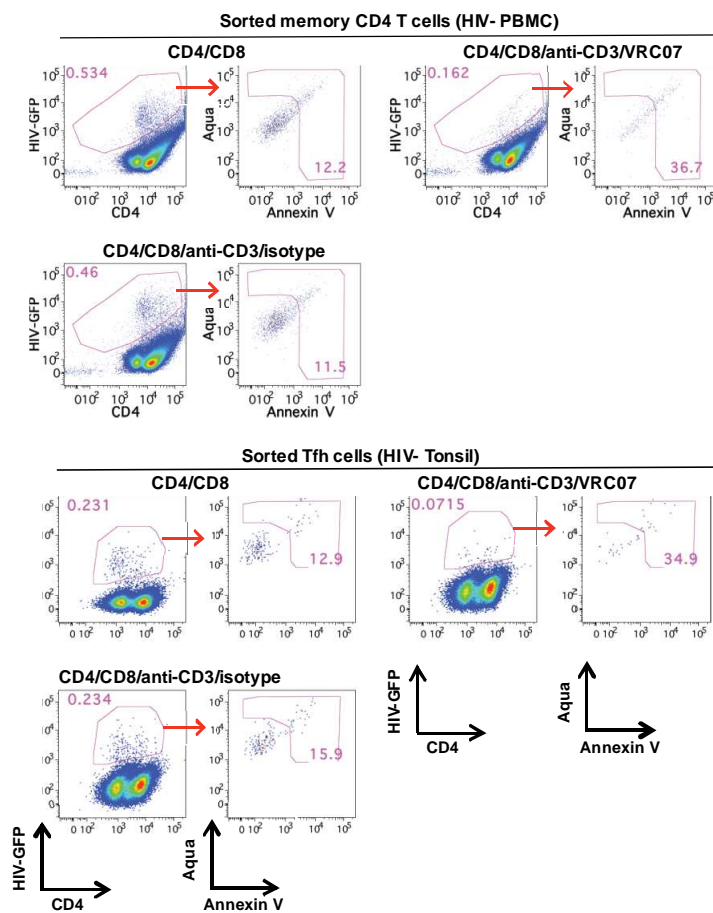
**A**



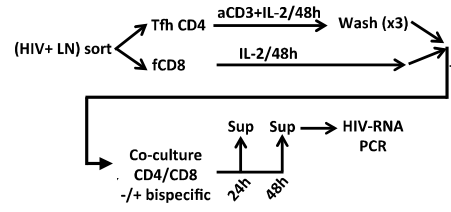
**B**



**C**



**D**



**E**

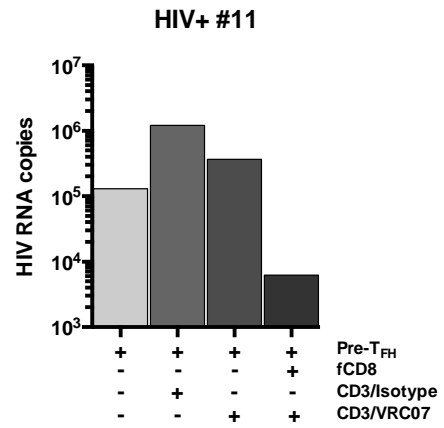




**Fig. S9. fCD8 T cells can mediate in vitro bispecific antibody killing.** (A) Schematic representation of the bispecific antibody and sorted CD8 T cell populations used in the *in vitro* killing assay. (B) Gating strategy to quantify the frequency of lysed HIV-infected cells (CEM) judged by the binding of Aqua and Annexin V. (C) Sorted primary memory CD4 T cells from HIV<sup>-</sup> PBMC (representative of two experiments) (*upper panel*) or T<sub>FH</sub> cells from HIV<sup>-</sup> tonsil (representative of three experiments) (*lower panel*) were infected *in vitro* with HIV encoding GFP and the frequency of HIV infected (GFP<sup>+</sup>) cells and the expression of apoptotic markers (Aqua and annexin V) in these cells after co-culture (8h) with autologous memory CD8 T cells in the absence or presence of bispecific antibodies is shown. (D) Schematic representation of the viral outgrowth assay used for sorted T<sub>FH</sub> cells and autologous fCD8 T cells from two viremic LNs. (E) Sorted PD-1<sup>dim</sup> pre-T<sub>FH</sub> cells from a viremic LN were stimulated *in vitro* (anti-CD3, 48h) and the virus production (judged by the HIV gag RNA copies) in the presence of bispecific antibodies or autologous fCD8 T cells and anti-CD3/VRC07 after 48h co-culture is shown.

**Table S1. Demographic (age and gender) and clinical (CD4 counts, pVL, and treatment) data of the donors as well as the type of assay used for their tissue analysis are shown.**

Code	Age (years)/ Gender	Diagnose (months)	CD4 T cells (cells/mm <sup>3</sup> )	Log <sub>10</sub> VL (copies/mL)	cART (months)	Analysis
HIV+ #1	30/M	50	591	4.58	Naïve	FACS/R/D
HIV+ #2	22/M	15	1136	4.66	Naïve	FACS
HIV+ #3	47/M	1	666	3.96	Naïve	FACS
HIV+ #4	23/M	1	199	3.48	Naïve	FACS
HIV+ #5	41/M	1	330	5.20	Naïve	FACS
HIV+ #6	29/M	55	734	3.90	Naïve	FACS
HIV+ #7	42/F	3	433	4.20	Naïve	FACS
HIV+ #8	31/M	12	671	4.15	Naïve	FACS/R/D
HIV+ #9	28/M	4	1288	4.46	Naïve	FACS/R/D
HIV+ #10	20/M	1	274	4.24	Naïve	FACS/R/D
HIV+ #11	26/F	15	304	3.26	Naïve	FACS/Cu
HIV+ #12	39/F	108	551	2.42	Naïve	FACS/Cu
HIV+ #13	23/M	2	428	4.68	Naïve	FACS
HIV+ #14	34/M	25	827	3.84	Naïve	FACS
HIV+ #15	36/M	6	335	5.26	Naïve	FACS
HIV+ #16	28/M	24	378	4.97	Naïve	FACS/F
HIV+ #17	21/M	6	574	4.02	Naïve	FACS
HIV+ #18	29/M	10	376	4.73	Naïve	FACS
HIV+ #19	27/M	2	752	4.65	Naïve	C/HC
HIV+ #20	28/M	3	261	4.96	Naïve	C/HC
HIV+ #21	34/M	1	355	4.93	Naïve	C/HC
HIV+ #7	42/F	3	433	4.20	Naïve	C/HC
HIV+ #22	31/M	1	334	5.31	Naïve	C/HC
HIV+ #23	19/F	1	566	4.09	Naïve	FACS
cART #1	35/M	101	393	2.05	15	FACS
cART #2	35/M	3	301	2.42	2.5	FACS
cART #3	42/M	48	243	1.95	1	FACS
cART #4	23/M	1	603	2.44	0.8	FACS
cART #5	31/M	21	419	1.60	21	FACS
cART #6	34/M	27	380	1.68	28 (2y)	FACS
cART #7	33/M	41 (3y)	1121	<1.6	25 (2y)	FACS/R/D
cART #8	44/M	192 (16y)	545	<1.6	84 (7y)	FACS/C/R/D
cART #9	58/M	228 (19y)	636	<1.6	180 (15y)	FACS/C/R/D
cART #10	57/M	348 (29y)	500	<1.6	204 (17y)	FACS/C/R/D
cART #15	51/M	204 (17y)	805	<1.6	120 (10y)	FACS/C
cART #14	37/M	60 (5y)	662	<1.6	48 (4y)	FACS
cART #11	28/M	9	580	1.6	8	C/HC
cART #12	49/M	7	834	1.6	4	C/HC
cART #13	34/M	45	491	1.79	7	C/HC
cART #16	34/M	3	301	2.42	2	C
cART #17	28/M	49	734	3.9	6	C
cART #18	22/M	1	603	2.44	1	C

\*cART – combined antiretroviral therapy; C – Confocal analysis; HC –Histo-cytometry analysis; R – HIV RNA quantification; D – gag DNA quantification; Cu – co-culture; F – fluidigm analysis